

A PARTIAL SHORT-FACED BEAR SKELETON FROM AN OZARK CAVE WITH COMMENTS ON THE PALEOBIOLOGY OF THE SPECIES

BLAINE W. SCHUBERT

Environmental Dynamics, 113 Ozark Hall, University of Arkansas, Fayetteville, AR 72701, and Geology Section, Research and Collections, Illinois State Museum, Springfield, IL 62703 USA

JAMES E. KAUFMANN

Department of Geology and Geophysics, University of Missouri-Rolla, Rolla, MO 65409 USA

*Portions of an extinct giant short-faced bear, *Arctodus simus*, were recovered from a remote area within an Ozark cave, herein named Big Bear Cave. The partially articulated skeleton was found in banded silt and clay sediments near a small entrenched stream. The sediment covered and preserved skeletal elements of low vertical relief (e.g., feet) in articulation. Examination of a thin layer of manganese and clay under and adjacent to some skeletal remains revealed fossilized hair. The manganese in this layer is considered to be a by-product of microorganisms feeding on the bear carcass. Although the skeleton was incomplete, the recovered material represents one of the more complete skeletons for this species. The stage of epiphyseal fusion in the skeleton indicates an osteologically immature individual. The specimen is considered to be a female because measurements of teeth and fused postcranial elements lie at the small end of the size range for *A. simus*. Like all other bears, the giant short-faced bear is sexually dimorphic. A review of *A. simus* records revealed that only small individuals have been recovered from cave deposits. This association of small *A. simus* specimens with caves suggests that females used these subterranean shelters for denning.*

In December 1998, Andy Free, a member of a cave mapping crew led by one of the authors (JEK), discovered the fragmentary remains of a large skeleton in the far reaches of a Missouri Ozark cave (Fig. 1). The survey crew was composed of members of the Missouri School of Mines Spelunkers Club from the University of Missouri-Rolla. This discovery led to a paleontological survey of the site in January 1999 by BWS. Following the preliminary identification of the specimen as *Arctodus simus*, excavations supported by the Illinois State Museum (ISM), the Missouri School of Mines Spelunkers Club, and the Cave Research Foundation, began in late February 1999. Due to logistical challenges associated with the site, excavations were not completed until March 2000. Here we present a description of this find from Big Bear Cave (BBC) and evaluate some aspects of the paleobiology of short-faced bears. A magazine article provided an informal account of this project (Schubert 2001).

SHORT-FACED BEARS

Although ursids first appear during the Miocene, their fossil record remains relatively meager until the Pleistocene. Two ursid subfamilies are represented in the New World, Tremarctinae and Ursinae. The earliest known tremarctine is the late Miocene *Plionarctos* (Tedford & Martin 2001). *Arctodus* appears during the Pliocene and is represented by *Arctodus pristinus* (lesser short-faced bear), a smaller, more gracile form with a proportionally longer snout than *A. simus* (giant short-faced bear) (Kurtén & Anderson 1980). Five species of short-faced bears have been described from the Pleistocene of South America (within the genus *Arctotherium*;

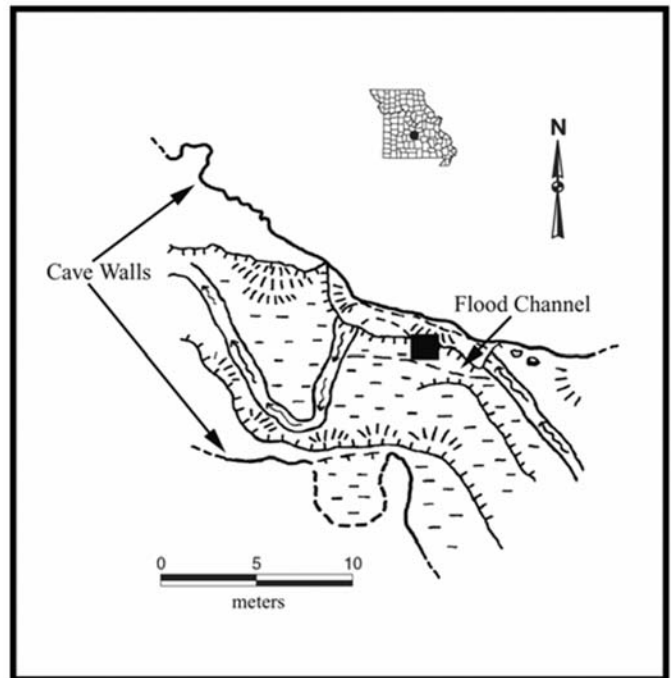


Figure 1. Map of Missouri showing location of Big Bear Cave (black dot) and plan view sketch showing the cave passage where *Arctodus simus* remains were discovered, ~1.4 km from the modern entrance. The excavated area is indicated by a black rectangle. NSS standard map symbols follow Hedges *et al.* (1979).



Figure 2. Articulated *Arctodus simus* forearms *in situ* and forearm of caver for scale.

Soibelzon 2002). Another tremarctine genus, *Tremarctos*, appeared during the late Pliocene in North America (Tedford & Martin 2001). The only living representative of the tremarctine subfamily is *Tremarctos ornatus* (spectacled bear) of South America.

Arctodus simus was the largest Pleistocene terrestrial carnivore in North America (Churcher *et al.* 1993; Christiansen 1999). Recent estimates of body weight based on bone proportions place *A. simus* as heavier than other extant and extinct ursids, with large individuals weighing at least 700 kg, and perhaps more than a metric ton on occasion (Christiansen 1999).

The giant short-faced bear previously was reported from over one hundred localities in North America, ranging from Mexico to Alaska and from the Pacific to the Atlantic coasts (Richards *et al.* 1996). Eight of these localities are Ozark caves (Hawksley 1965; Hawksley 1986; Hawksley *et al.* 1973; Puckette 1976; Hawksley & Weaver 1981; Schubert 2001). Temporally this species ranged from the middle Irvingtonian North American Land Mammal Age (NALMA) through the Rancholabrean NALMA, becoming extinct near the end of the Pleistocene in an extinction event that killed off most large North American mammals (Grayson 1989; Kurtén & Anderson 1980).

MATERIALS AND METHODS

Excavation was carried out during the winter months to avoid contact with the extensive gray bat (*Myotis grisescens*) maternity colony located between the entrance and the excavation site. Reaching the bear bones required a great deal of crawling and wading through streams and muddy crawlways. A typical excavation round trip lasted from 13-16 hours. For these reasons, the skeleton was exposed (Fig. 2), mapped (Fig. 3), and divided into sections that were removed from the cave in plaster jackets. Quick setting plaster bandages were used for the removal process. Only remains that could be removed in a single trip were excavated at one time. In all, 13 excavation trips were made to the short-faced bear locality.

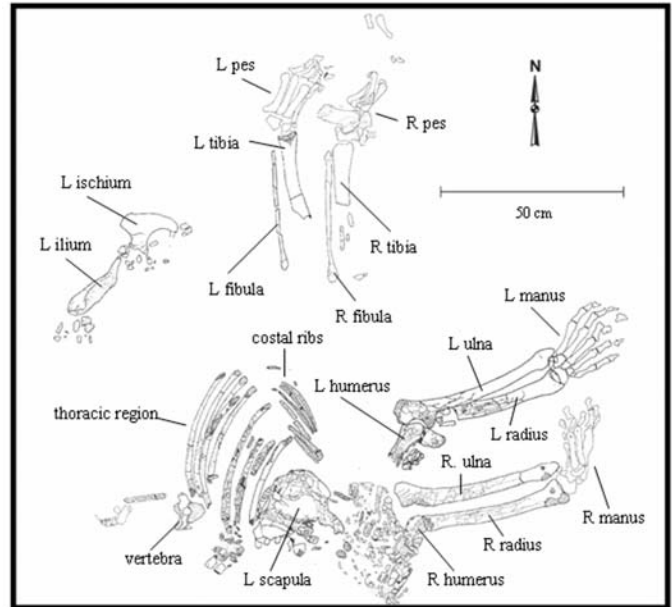


Figure 3. Plan view sketch of the excavated area showing *Arctodus simus* skeletal material *in situ*. Loose disturbed surface bones and teeth not shown on sketch.

The inner portions of BBC are typical of many caves in the central Ozarks, having streams, slick clay sediments, large sediment banks, and a constant high humidity. These characteristics present logistical challenges for excavation. All bone at the site was saturated and most of the material was highly fragmentary. Adhering to the bones was wet, sticky sediment, which proved difficult to remove without the sediment pulling off bone fragments.

The bear site (Figs. 1 & 3) was mapped by using survey station F9 from the original cave survey as a primary datum. This datum is a rock (with F9 written on it) located on a ledge above the excavation site. A secondary datum (a survey flag) was placed in the floor near the bear remains and is still in place. This secondary datum was used for vertically and horizontally mapping the skeleton with a tape measure, string, and line-level. Because of the poor condition of the skeletal material and distance from the cave entrance, plaster jackets were used to stabilize and transport most of the remains out of the cave. These plaster jackets were then transported to the ISM and prepared in the laboratory. Some of the remains were exposed but not removed from the sediment. These are currently conserved in plaster jackets (for example, see Fig. 4). Butvar™ was used as the consolidant for preserving nearly all the remains. Molds and casts of much of the articulated skeleton were also made in the ISM preparation laboratory. Digital calipers were used for measuring the smaller remains and sliding metal calipers for the larger specimens. Where possible, dimensions follow Merriam and Stock (1925), Kurtén (1967), and Driesch (1976). Length and width for dental measurements were taken at the base of the enamel. Skeletal and dental measurements are reported in millimeters (mm). All



Figure 4. Plaster jacket opened to show articulated left manus of *Arctodus simus*. White scale bar = 1 cm.

remains collected are now curated in the Geology Collections at the ISM under catalog number ISM 496850.

Scanning electron microscope (SEM) images were taken, and the energy dispersion spectrum (EDS) analysis was performed, at the Electron Microscopy Laboratory at UMR. X-ray diffraction analyses (XRD) were carried out in the Geochemistry and Clay Mineralogy Lab at UMR. Bone chemistry was analyzed at Stafford Laboratories, Boulder, Colorado, but, as noted below (under Chronologic Age), the specimen lacked sufficient bone protein for dating. Computed tomography (CT) scans were performed at Memorial Medical Center, Springfield, Illinois.

LOCALITY

Big Bear Cave formed in the Ordovician Gasconade dolomite. The entrance to the cave faces south and lies at the base of an 11 m tall bluff at the top of a steep slope ~26 m above the Gasconade River in Pulaski County, Missouri. The entrance is 25 m wide by 7 m high but the entrance passage narrows to 6 m wide by 3 m high after 55 m and soon becomes a crawlway only 1 m high. The layout of the cave is a series of 3 north-northwest-trending trunk passages connected by crawlways. The *Arctodus* remains were in a side passage (now termed "Arctodus Avenue"), ~150 m from the Bat Room and 1400 m from the current entrance of the cave. The Bat Room is the site of a large maternity colony of gray bats (*Myotis grisescens*) that roost in at least 5 separate locations. Arctodus Avenue continues for ~380 m, ending at a large rubble pile that blocks the passage. This appears to be the closest potential entrance that the short-faced bear might have used. Many side passages have not been mapped or explored and, the total length of all the cave passages is certainly much longer than the currently known 6500+ m length.

A cursory paleontological survey of a small portion of the cave by the authors revealed numerous black bear (*Ursus americanus*) bones, bear beds, claw marks, tracks, and possi-

ble bear scat. Further investigation is needed to better understand the use of the cave by bears. The cave is currently closed to all visitations by the landowners. To respect the owner's wishes for privacy we renamed the cave for this publication. The exact location and other names for the cave are on file in the Geology Section archives at the ISM and the Missouri Speleological Survey database, Missouri Department of Natural Resources, Geological Survey and Resource Assessment Division, Rolla, Missouri.

DEPOSITIONAL SETTING

The passage where the *Arctodus simus* specimen was located is ~10 m wide and 3 m high. The entrenched stream flows in a channel along the north wall where the ceiling along that side of the passage lowers to within 1 m of the stream. A sediment bank rises some 1 m from the stream bed level to the ceiling level and forms a 2 m wide terrace at that level before another 1 m high slope. Immediately downstream from the site, the sediment bank rises abruptly to meet the descending ceiling level, thus constricting the stream in a small ~75 cm wide by ~50 cm high tunnel. This constriction forces flood waters to overflow the stream channel and flow on the terrace level, which serves as a flood-overflow channel (Fig. 1).

Excavation showed the bear to be lying on its right side (Fig. 3) with the distal portions of the hind limbs located on a sloping floor near the modern stream level beneath the overhanging ledge. Much of the surface in the excavation area was covered by highly fragmented and water saturated bone. The majority of the skeleton was located on a flood overflow channel that previously served as a footpath for cavers. The hind limbs were located on the sloping surface with the feet lying ~25 cm below the thoracic region. The hind feet were buried under ~20 cm of sediment while the thoracic region was buried by only a few centimeters of sediment.

The sediment immediately below and encasing the carcass is composed of banded silt and silty clay composed predominantly of quartz (Fig. 5). This banded sediment is only a few centimeters thick in the flood overflow channel but thickens to nearly 40 cm at the base of the bank near the stream. The banded sediment overlies a poorly consolidated, predominately red clay (7.5YR 4/4) unit (all Munsell colors were judged using dried sediments). The lower portion of the banded sediments is tinted red by inclusions of silt-sized clay particles, which are apparently eroded fragments of the red clay. The upper portion of the sediment immediately below the carcass is composed of light (10YR 7/4) and dark (10YR 6/4) tan layers with occasional thin reddish layers. The hind limbs, being lower in elevation, were subjected to more frequent flooding and hence were buried more rapidly and to a greater thickness than the torso.

Intimately associated with the skeleton is a prominent discontinuous layer from 1-2 mm thick containing a black (N 2.5/0) mineral (Fig. 5, white arrows). This black layer is composed of small tubules and strands (Fig. 6) that we interpreted



Figure 5. Cross-sectional view of sediments below ribs. White arrows indicate manganese deposits containing hair molds and casts.

to be hair. In many places an unstratified brown (10YR 5/3) sediment averaging 10 mm thick overlies the black layer. Associated with this layer are occasional clumps of red clay that match the most common older sediments in the cave. These clumps often contain nodules of the black mineralization. Like the thin black layer noted above, the nodules contain tubules and strands that appear to be fossil hairs (see Systematic Paleontology). EDS analysis indicates that the primary constituent of this black layer is manganese (Fig. 7) while XRD analysis failed to indicate any major crystalline component. This is typical of fine-grained manganese oxide/oxy-hydroxide mixtures. We suggest that the clumps of red clay containing the larger manganese nodules with fossil hair were enmeshed in the hair prior to, or near the time of, the bear's death.

Several authors (Nealson *et al.* 1992; Nealson & Stahl 1997; and Tebo *et al.* 1997) reported on the deposition of manganese oxide and oxy-hydroxides by microbial oxidation processes. The manganese oxide and oxy-hydroxide layer associated with the *A. simus* skeleton may have occurred during microbial decomposition of the decaying carcass. The cave stream, sediments, and carcass itself are potential sources of the manganese. The amount of potential manganese available from the bear and sediments has not been calculated. However, Imes *et al.* (1996) reported that typical spring water in the region of BBC contains from 1-3 µg/L of manganese, suggesting that the stream alone could have supplied the manganese. This process of microbially moderated manganese deposition may help explain the relatively common black staining on paleontological remains from wet caves.

CHRONOLOGIC AGE

A fragment of an incisor root was sent to Stafford Research Laboratories, Inc., Boulder, Colorado. Pretreatment techniques (Stafford *et al.* 1987; Stafford *et al.* 1991) indicated that the specimen had a non-collagenous amino acid composition containing 3nm/mg of protein, 0.1% of the protein found in modern tooth samples. Therefore, an AMS radiocarbon date attempt was not justified because of the low protein content of the dentine. This leaching of protein from the skeletal remains was probably the result of periodic inundation. Although an exact age could not be determined for the *A. simus* specimen, a Rancholabrean age is inferred based on the known time range of this species.

SYSTEMATIC PALEONTOLOGY

- Order Carnivora Bowdich, 1821
- Family Ursidae Gray, 1825
- Subfamily Tremarctinae Kraglievich, 1926
- Genus *Arctodus* Leidy, 1854
- Arctodus simus* (Cope), 1879
- (Giant Short-faced Bear)
- (Figs. 6 and 8; Tables 1-5)

Table 1. Measurements of *Arctodus* teeth. Dimensions after Driesch (1976) and Merriam and Stock (1925). (1) = M2 length dimension as in Driesch, (2) = M2 length dimension perpendicular to the midline. Observed ranges (OR) for *Arctodus pristinus* and *Arctodus simus* from Emslie (1995) and Richards *et al.* (1996). X = comparative measurements not reported in Richards *et al.* (1996). * = M2s may have been measured using either methodology noted here (1 or 2).

Measurement	BBC specimen	<i>Arctodus pristinus</i> OR (N)	<i>Arctodus simus</i> OR (N)
i2			
greatest transverse diameter	L 8.3, R 8.4	X	X
i3			
greatest transverse diameter	L 11.0	X	X
p4			
anteroposterior diameter	R 13.3	10.5-12.2 (9)	10.3-13.7 (13)
greatest transverse diameter	R 8.5	6.7-7.5 (7)	6.2-8.8 (12)
m1			
anteroposterior diameter	R 32.8	24.3-29.5 (15)	29.6-35.3 (32)
greatest transverse diameter of anterior half	R 16.1	X	X
greatest transverse diameter of heel	L 15.9, R 15.8	13.0-15.7 (15)	15.1-18.4 (6)
m2			
anteroposterior diameter	R 30.8	22.6-28.7 (18)	26.3-33.6 (45)
greatest transverse diameter	R 20.8	X	X
m3			
anteroposterior diameter	L 21.7	16.1-22.5 (14)	18.7-24.2 (33)
greatest transverse diameter	L 17.1	13.5-17.0 (14)	14.5-19.1 (33)
I1			
greatest transverse diameter	L 9.0, R 8.9	X	X
I2			
greatest transverse diameter	R 10.0	X	X
I3			
greatest transverse diameter	R 13.3	X	X
M2			
anteroposterior diameter (1)	R 38.5		
anteroposterior diameter (2)	R 37.3	*33.0-39.0 (9)	*33.3-42.9 (42)
greatest transverse diameter (anterior width)	R 22.8	19.6-22.5 (9)	20.8-26.6 (42)

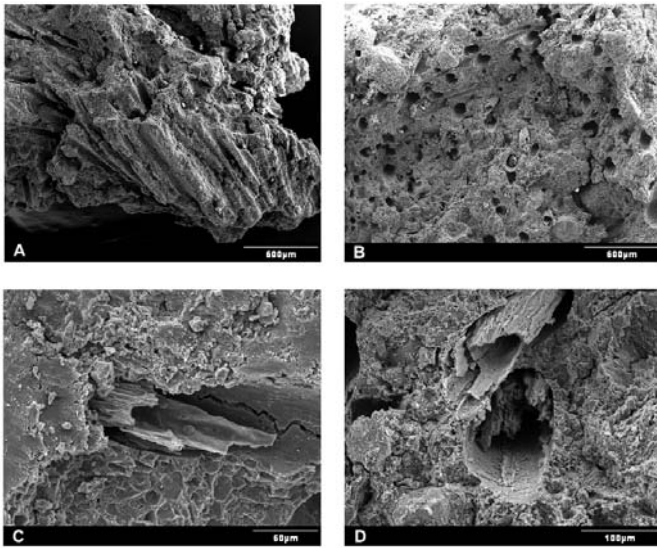


Figure 6. Scanning electron micrographs of *Arctodus simus* fossilized hair. A, hair molds; B, cross-sectional view of hair molds and hair; C and D, close-up of individual molds and hair.

Table 2. Measurements of *Arctodus* calcanea and metacarpals. Dimensions after Driesch (1976). For the BBC specimen the greatest breadth of the distal end of the metacarpals was taken perpendicular to the shaft, not at an angle as shown in Driesch (1976). This measurement was taken at the widest point of the distal end, which is the contact between the shaft and the epiphysis. Observed ranges (OR) for *Arctodus pristinus* and *Arctodus simus* from Richards *et al.* (1996). X = comparative measurements not reported in Richards *et al.* (1996). * = pathological.

Measurement	BBC specimen	<i>Arctodus pristinus</i> OR (N)	<i>Arctodus simus</i> OR (N)
calcaneus			
greatest length	L 108.5, R 108.4	99.0 (1)	101.0-136.0 (16)
greatest width	L 72.4, R 71.7	65.0 (1)	67.0-92.8 (14)
metacarpal I			
greatest length	R 75.1	70.0 (1)	73.5-100.0 (10)
greatest breadth of distal end	R 19.2	18.7 (1)	17.4-27.2 (10)
metacarpal II			
greatest length	R 103.3	X	97.0-135.0 (9)
greatest breadth of distal end	R 24.4	X	23.5-34.0 (9)
metacarpal III			
greatest length	R 109.5	96.0 (1)	104.0-142.0 (10)
greatest breadth of distal end	R 24.4	22.9 (1)	24.8-35.4 (10)
metacarpal IV			
greatest length	*R 110.6	100.0 (1)	107.0-133.2 (8)
greatest breadth of distal end	*R 26.1	25.3 (1)	23.5-33.7 (8)
metacarpal V			
greatest length	R 111.1	X	98.0-130.0 (7)
greatest breadth of distal end	R 27.3	X	23.0-34.2 (7)

MATERIAL

All the remains are cataloged within the same number, ISM 496850. The recovered elements include whole or partial specimens of L i2; R i2; L i3; R p4; L m1 fragments; R m1; R m2; L m3; L I1; R I1; R I2; R I3; R M2; enamel cap of p2/P2 or p3/P3; two M1? fragments; vertebral epiphyses; portions of 2 thoracic vertebrae; rib epiphyses; rib fragments; portions of at least 7 costal ribs; portions of L ilium and ischium; portions of L, R scapulae; L, R humeri, distal ends; L, R ulnae; L, R radii; L, R pisiforms; L, R scapholunars; L, R cuneiforms; L, R unciforms; L, R trapezoids; L, R trapeziums; L, R metacarpals I-V;

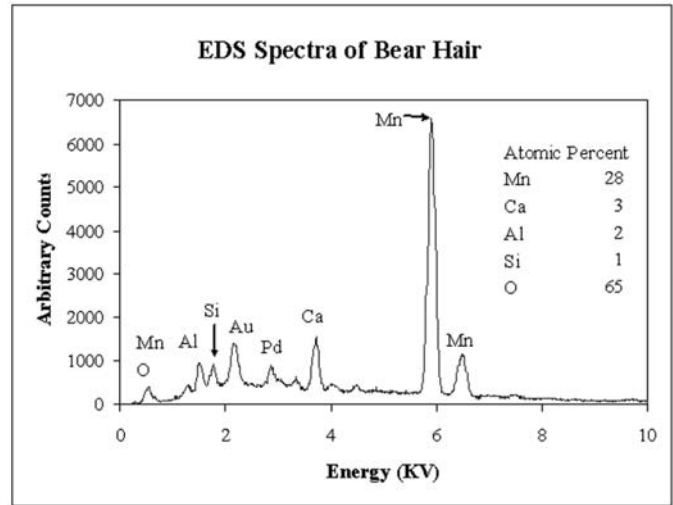


Figure 7. Energy Dispersal Spectral analysis (EDS) on black sediment containing fossil bear hair. Gold (Au) and palladium (Pd) were used to coat the sample to make it electrically conductive.

Table 3. Measurements of Big Bear Cave *Arctodus simus* proximal and middle phalanges, right manus. Dimensions after Driesch (1976).

Measurement	BBC specimen
proximal phalanx, digit II	
greatest length	49.0
greatest breadth of proximal end	25.2
least breadth of diaphysis	14.0
greatest breadth of distal end	18.7
proximal phalanx, digit III	
greatest length	51.2
greatest breadth of proximal end	25.8
least breadth of diaphysis	14.7
greatest breadth of distal end	19.6
proximal phalanx, digit IV	
greatest length	54.3
greatest breadth of proximal end	27.5
least breadth of diaphysis	15.4
greatest breadth of distal end	20.5
proximal phalanx, digit V	
greatest length	52.6
greatest breadth of proximal end	26.4
least breadth of diaphysis	14.1
greatest breadth of distal end	19.1
middle phalanx, digit II	
greatest length	36.2
greatest breadth of proximal end	19.9
least breadth of diaphysis	13.6
greatest breadth of distal end	18.1
middle phalanx, digit IV	
greatest length	38.7
greatest breadth of proximal end	20.5
least breadth of diaphysis	12.2
middle phalanx, digit V	
greatest length	34.5
greatest breadth of proximal end	19.9
least breadth of diaphysis	12.5
greatest breadth of distal end	16.7

L proximal phalanges of manus digits I-V; R proximal phalanges of manus digits II-V; L medial phalanges of manus digits II-V; R medial phalanges of manus digits II, IV, and V; L terminal phalanges of manus digits I-V; four R terminal manus phalanges (undifferentiated); 10 sesamoids from L manus; 8

Table 4. Measurements of *Arctodus* right and left metatarsals. Dimensions after Driesch (1976). Observed ranges (OR) for *Arctodus pristinus* and *Arctodus simus* from Richards *et al.* (1996).

Measurement	BBC specimen	<i>Arctodus pristinus</i> OR (N)	<i>Arctodus simus</i> OR (N)
metatarsal I			
greatest length	L 74.6	66.0 (1)	71.0-84.0 (7)
greatest breadth of distal end	L 18.0	17.7 (1)	16.7-25.0 (8)
metatarsal II			
greatest length	L 94.7	80.0-90.0 (2)	86.0-101.3 (3)
greatest breadth of distal end	L 23.6	22.4-23.0 (2)	23.6-25.6 (4)
metatarsal III			
greatest length	L 103.4, R 103.4	90.0-106.0 (2)	94.0-124.1 (12)
greatest breadth of distal end	L 23.3, R 24.2	24.2 (1)	23.2-35.8 (12)
metatarsal IV			
greatest length	L 114.1, R 114.1	98.0 (1)	105.0-132.3 (6)
greatest breadth of distal end	L 24.9, R 25.2	24.0 (1)	23.5-35.1 (6)
metatarsal V			
greatest length	L 113.1	98.0 (1)	85.0-135.0 (11)
greatest breadth of distal end	L 25.7	22.0 (1)	18.3-31.4 (11)

Table 5. Measurements of Big Bear Cave *Arctodus simus* proximal and middle pes phalanges. Dimensions after Driesch (1976).

Measurement	BBC specimen
proximal phalanx, digit I	
greatest length	L 39.5
greatest breadth of proximal end	L 19.6
least breadth of diaphysis	L 12.0
greatest breadth of distal end	L 14.8
proximal phalanx, digit II	
greatest length	L 39.9
greatest breadth of proximal end	L 22.8
least breadth of diaphysis	L 13.9
greatest breadth of distal end	L 16.2
proximal phalanx, digit III	
greatest length	L 42.2
greatest breadth of proximal end	L 23.1
least breadth of diaphysis	L 14.3
greatest breadth of distal end	L 17.3
proximal phalanx, digit IV	
greatest length	L 48.4
greatest breadth of proximal end	L 25.1
least breadth of diaphysis	L 14.6
greatest breadth of distal end	L 18.0
proximal phalanx, digit V	
greatest length	L 45.7
greatest breadth of proximal end	L 23.4
least breadth of diaphysis	L 12.6, R 12.7
middle phalanx, digit II	
greatest length	L 28.1
greatest breadth of proximal end	L 18.5
least breadth of diaphysis	L 13.0
greatest breadth of distal end	L 15.6
middle phalanx, digit III	
greatest length	L 30.7
greatest breadth of proximal end	L 19.0
least breadth of diaphysis	L 12.3
greatest breadth of distal end	L 16.2
middle phalanx, digit IV	
greatest length	L 32.4
greatest breadth of proximal end	L 19.6
least breadth of diaphysis	L 12.1
greatest breadth of distal end	L 15.9
middle phalanx, digit V	
greatest length	L 29.1
greatest breadth of proximal end	L 18.8
least breadth of diaphysis	L 12.0
greatest breadth of distal end	L 15.2

sesamoids from R manus; proximal end of L femur; proximal shaft of R femur; L, R patellae; L, R tibiae, proximal and distal portions for both sides; fragmentary L fibula; R fibula; L, R calcanea, L, R astragali; L, R mesocuneiforms; L, R naviculars; L, R ectocuneiforms; L, R entocuneiforms; L, R cuboids;

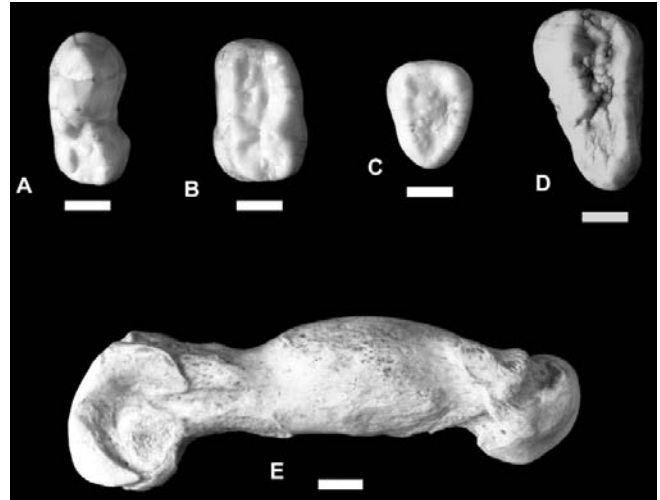


Figure 8. Selected elements from the BBC *Arctodus simus* skeleton. All teeth are shown in occlusal view. A, R m1; B, R m2; C, L m3; D, R M2. E, pathological R metacarpal IV. White scale bars = 1 cm.

L, R metatarsals I-V; L proximal phalanges of pes digits II-V; L medial phalanges of pes digits I-V; L terminal phalanges of pes digits I-III and V; R proximal phalanx of pes digit V; R terminal phalanx of pes digit V; 10 sesamoids from L pes; 3 sesamoids from R pes; one undifferentiated sesamoid; numerous bone and tooth fragments; sediment samples with fossilized hair and hair casts in manganese.

DIAGNOSIS

Tremarctine bears can be morphologically distinguished from ursine bears based on the presence of a premesetetic fossa on the mandible, an entepicondylar foramen on the humerus, and an extra lateral cusp between the talonid and trigonid on the m1 in the former (Kurtén & Anderson 1980). Although the dentaries and significant portions of the distal humeri were not recovered from the BBC specimen, the preserved R m1 has the extra lateral cusp aforementioned. Identification beyond the subfamily level has relied mostly on size differences. The genus *Arctodus* has higher crowned and considerably larger teeth than *Tremarctos*. *Arctodus pristinus* is distinguished from *A. simus* by its lesser size, greater prognathism, and smaller, narrower, and less crowded teeth (Kurtén & Anderson 1980; Emslie 1995). *Arctodus simus* is highly variable in size with the lower end of the observed range overlapping with *A. pristinus* in many measurements (Kurtén 1967; Richards *et al.* 1996). However, Kurtén (1967) concluded, and others have followed suit (e.g., Emslie 1995; Richards *et al.* 1996), that it is possible to distinguish *A. simus* from *A. pristinus* based on measurements and proportions of the teeth. Unfortunately, sample sizes for *A. pristinus* elements remain small (Richards *et al.* 1996: Appendix 2). Nevertheless, compared to compiled dental measurements (from Emslie 1995 and Richards *et al.* 1996), the BBC specimen is consistently within the range of *A. simus*, and 7 of the 9 measurements

taken lie above the range of *A. pristinus* (Table 1). Measurements on other skeletal elements also group the BBC specimen as a small *A. simus* (Tables 2 & 4).

DESCRIPTION

TEETH: No cranial or mandibular bones were identified from the site and the teeth were isolated and scattered. Numerous pieces of enamel were recovered, as well as root fragments. Tooth enamel is well preserved but the roots were saturated, fragmented, and have a purplish hue. The lack of tooth-bearing elements and cranial material is the likely result of long-term exposure of these remains in a depositional system with very slow sediment accumulation rates and a high humidity. A thin layer of clay and degraded bone on the current surface covered the teeth.

No hypoplasias or dental caries were found. However, supragingival dental calculus is relatively common and is present on most of the recovered teeth. This feature is most noticeable on the cheek teeth; the best example is seen on the R m2, where nearly half the labial surface is covered with supragingival calculus. Much of the calculus appears to have exfoliated over time; thus, the calculus that remains does not represent the exact coverage of calculus at the time of death.

Occlusal wear on the teeth is minimal (Fig. 8), but is described here for future comparison. Measurements of the dentine exposures are made from contact lines between the dentine and enamel on the occlusal surfaces. The L i2 has two wear facets with exposed dentine. The larger facet is more medially placed and has a maximum labiolingual width of 2.2 mm and a maximum mesiodistal width of 4.5 mm. The smaller facet with exposed dentine is near the lateral margin of the tooth. It has a maximum labiolingual width of 1.0 mm and a maximum mesiodistal width of 1.1 mm. The R i2 also has two wear facets with exposed dentine. The larger facet has a labiolingual maximum width of 2.0 mm and mesiodistal maximum width of 2.0 mm. The smaller wear facet is in contact with the lateral margin of the tooth and has a maximum labiolingual width of 2.0 mm and a mesiodistal width of 1.1 mm. On the R i3 dentine is exposed on the larger more proximal cusp but not on the smaller more lateral cusp. The maximum labiolingual width of the dentine on the larger cusp is 2.0 mm and the maximum mesiodistal width is 5.0 mm. The R p4 and the enamel cap (p2/P2 or p3/P3) displayed no wear facets with exposed dentine and appeared to be relatively unworn. The L m1 is not complete. The represented portion shows some wear and dentine exposure. The large protoconid has a wear facet with a maximum mesiodistal width of 1.5 mm and a maximum buccolingual width of 2.0 mm. The portion of the tooth containing the lateral accessory cusp was not recovered from the cave. The R m1, like the L m1, has a wear facet on the apex of the protoconid (Fig. 8A). The mesiodistal maximum width of the dentine exposure is 1.4 mm and the buccolingual exposure is 1.6 mm wide. The lateral accessory cusp between the trigonid and talonid also shows minor wear, with the mesiodistal maximum width of the facet being 1.5 mm and a buccolingual maximum width of 0.6 mm. The R m2 (Fig. 8B) and L m3 (Fig.

8C) displayed no wear facets with exposed dentine and the teeth are relatively unworn.

Like the lower dentition, some of the upper teeth show wear, and the most extreme is on the incisors. The L I1 has one relatively large wear facet with exposed dentine. The labiolingual maximum width is 4.2 mm and the mesiodistal maximum width is 6.5 mm. At least one diminutive wear impression was apparent on a small cusp posterior and medial to the larger wear facet. The R I1 has one large wear facet with a labiolingual maximum width of 4.5 mm and a mesiodistal width of 6.6 mm. One smaller cusp, posterior and medial to larger cusp, has a small wear facet with a labiolingual maximum width of 0.5 mm and a mesiodistal maximum width of 0.6 mm. There is also a groove on the occlusal surface approximately 4.5 mm long and 0.5 mm wide that was not on the LI1. This attritional groove is u-shaped in cross-section, runs labiolingually, and is along the lateral margin of the occlusal surface. The R I2 has one large wear facet with a labiolingual maximum width of 3.5 mm and a mesiodistal length 6.4 mm. The R I3 has a wear facet with exposed dentine. The labiolingual maximum width is 1.0 mm and the mesiodistal width is 1.0 mm. The L M1? fragments and the R M2 (Fig. 8D) did not have any exposed dentine/wear facets and appeared to have little to no wear.

VERTEBRAE: The vertebral elements recovered consist of spinous and transverse processes, vertebral body fragments lacking epiphyses and isolated unfused vertebral epiphyses. One partial thoracic vertebra is curated with the surrounding sediment holding the specimen together.

RIBS: The ribs were smashed, cracked, and in very poor condition but many were preserved in sequence. This high level of fragmentation is probably the result of people walking over the site. Like the vertebral elements, these remains were near the modern surface (3-5 cm depth). All of the long rib segments lacked proximal articular ends. Some of these proximal ends were recovered and the proximal epiphyses were not fused at the time of death. Due to their poor condition nearly all the rib segments have been preserved within the original sediments. At least 7 segments of calcified costal cartilage were also recovered in sequence. These too have been preserved in their original position within matrix.

SCAPULAE: Both scapulae are highly fragmented and curated with matrix holding them together. The L scapula is on top of the left side of the ribcage and at least 4 ribs are preserved underneath it. The R scapula was in a semi-articulated position.

HUMERI: The distal half of the R humerus is represented by a block of sediment and highly degraded bone. Portions of the remaining distal end were articulated with the R ulna and radius. The L humerus is in poor condition, but the distal portion was articulated to the L ulna and radius.

ULNAE AND RADII: The L and R ulnae and radii are nearly complete. The shafts and proximal ends are highly fragmented, but the distal ends are intact. The proximal epiphyses on the ulnae could not be examined because of the poor preservation of these areas. On both distal ulnae, the epiphyseal suture is visible only on the radial surface. The epiphyseal sutures on

the distal radii are faint but visible.

MANUS: The L and R ulnae were articulated with their corresponding carpals. All epiphyseal plates in the metacarpals and phalanges are completely fused. The L manus was splayed out with palm down and was preserved in an articulated position within sediment. The second phalanx of digit II was out of orientation on the L manus and was discovered to be under the terminal phalanx of the same digit based on a CT scan. The CT scan also showed that the sesamoids between the metacarpals and phalanges are in their natural position within the sediment. The R manus was also articulated but was not complete. Its slightly higher position on the paleosurface and orientation made it more susceptible to erosion and disturbance than the L manus. The L manus is currently curated in sediment (see Fig. 4). The R manus was found on its side, with digit V being the lowest and digit I lying across the palm in a semi-closed position. The R fourth metacarpal possesses a well healed fracture (Fig. 7E). The R manus was also CT scanned to preserve the natural position of the bones prior to removal from the encasing sediments.

INNOMINATE: These remains were curated within sediment. Much of the L ischium is well preserved and some L iliac fragments are identifiable. The ischial tuberosity epiphysis is in contact with the ischium but is not fused. The acetabulum is obliterated. Additional innominate fragments were recovered from the disturbed surface area.

FEMORA AND PATELLAE: The proximal end of the L femur was found buried just west of the majority of the skeleton underneath a block of red clay. The recovered proximal end includes a small portion of the diaphysis and the complete fused capitular epiphysis. Although the epiphysis adheres to the diaphysis, the deep suture separating these parts indicates that fusion was in progress at the time of death.

The proximal end of the R femur shaft was recovered from the surface. The coloration of the fracture surfaces on the femur, and many other surface bones, indicated that these breaks were likely the result of earlier cavers. The recovered R femur lacks the capitular epiphysis, again indicating that this was an osteologically immature individual. The greater trochanter epiphysis is fused but the suture line is still visible. Both the L and R patellae were recovered from the surface near the R femur shaft and are complete.

TIBIAE/FIBULAE: The proximal ends of the L and R tibiae were recovered from the surface near the R femur and the patellae. Both tibiae have cut marks on the proximal ends. The much lighter coloration of these cut mark surfaces, compared to intact surfaces, indicates that other cavers discovered the site at some point in the recent past and some digging occurred.

The distal ends of the tibiae and fibulae were still articulated in sediments near the stream. The epiphyses are fused on the proximal R tibiae but a clear suture still exists along some portions of the contact. The distal epiphysis on the R tibia is completely fused and no suture line is visible. The stage of fusion of the proximal L tibia mirrors that observed on the R

tibia. The distal epiphysis on the L tibia is well fused and the suture line is only visible in one location along the lateral surface. The fibulae are nearly identical in their stage of epiphyseal closure. The distal epiphyses are completely closed and the proximal epiphyseal sutures are still visible, particularly on the lateral sides.

PES: The tarsals were articulated with their corresponding tibiae and fibulae. All epiphyses in the metatarsals and pedal phalanges are fused. The L pes was found articulated with the ventral side down. It is nearly complete and was CT scanned prior to removal of the surrounding sediment to record the original orientation of the foot. The R pes was partially articulated and lying on its lateral side, thus digit V was the lowest. Because of this orientation, most of the medial and central phalanges washed away prior to burial.

HAIR: As noted above, we interpreted tubular structures as *Arctodus simus* hair molds and hair. Scanning electron microscopy (SEM) revealed that these tubules and strands have a structure and size similar to hair (Fig. 6). These structures overlap one another but do not branch or intersect and were recovered only from beneath or right next to the bear's skeletal remains. The hydrophobic keratinaceous protein composition of hair is not easily degraded when compared to other soft tissues (Rowe 1997). Thus, the preservation of hair features near the articulated skeletal remains should not be overly surprising. Unfortunately, the fossilized hair material we analyzed was too degraded to retain the scale pattern of the surface, texture, and morphology of distinct regions, and diameter of the medulla. Numerous blocks of sediment containing fossilized hair are preserved and are available for further analysis.

DISCUSSION

We can only speculate about what caused the death of this relatively young bear in the depths of this cave. Other than the healed metacarpal fracture, there was no sign of trauma on the skeletal remains. The only evidence of disease is extensive supragingival calculus on some of the cheek teeth, but this is not a life-threatening condition.

The BBC *A. simus* specimen was not osteologically mature when it died because numerous epiphyses were unfused. However, the stage of fusion of the long bone epiphyseal plates indicate that this animal was, for the most part, full sized. The age of individual modern bears can be determined using a number of methods. The most reliable technique used by neontologists studying older individuals in modern bear populations is counting cementum annuli on thin-sectioned premolars and canines (Harshyne *et al.* 1998). Though cementum annuli analysis may prove useful in understanding the paleobiology of short-faced bears in the future, at this point no specimens have been aged using this destructive technique.

Because the BBC specimen is osteologically immature, comparisons with known epiphyseal fusion sequences in extant bears may be made. Epiphyseal closures of the fore-

limbs in *Ursus americanus* are discussed by Marks and Erickson (1966) as a tool for determining age. X-rays of known-age *U. americanus* showed that the stages of the closure of the long bone epiphyses and the development of the carpals are closely correlated to age (Marks & Erickson 1966). They found that the metacarpal epiphyses fused in both sexes around the age of 1-2 years and the proximal and distal epiphyses fused on the ulna and radius in females around the age of 4-6 years (6-8 years in males). At present it is not known whether *Arctodus* had a similar rate and sequence of epiphyseal fusion to any of the genus *Ursus*. However, on the basis of fusion rates and sequences in black bears, the BBC *Arctodus simus* may be placed at around 4-6 years of age if it is a female and around 6-8 if it is a male. Interestingly, the wear patterns on the BBC bear's teeth is similar to 4-6 year old black bears (Marks & Erickson 1966). Unfortunately no comparable data exists for the extant tremarctine, *Tremarctos ornatus*.

The late time of epiphyseal fusion noted above indicates that bears are sexually mature well before their epiphyseal fusions are complete. If short-faced bears were similar in their timing of sexual maturity to modern bears, the BBC specimen would have been sexually mature. Female *T. ornatus* reach sexual maturity as early as 4 years of age (Stirling 1993a). Extant North American bears follow a similar pattern. For example, female black bears become sexually mature between 2 and 4 years of age (Larivière 2001; Stirling 1993a) and female brown or grizzly bears (*Ursus arctos*) begin breeding in some portions of their range at around 3 years (Pasitschniak-Arts 1993).

The postcranial remains of *A. simus* described here are at the small end of the recorded size range (Tables 1, 2 & 4). Kurtén (1967), Harington (1991), and Richards *et al.* (1996) divide *A. simus* into 2 subspecies, small *A. s. simus* and large *A. s. yukonensis*. Lamb (1911) and Voorhies and Corner (1982) suggested a specific rather than a subspecific distinction for the large and small forms. It is now generally accepted that all of these specimens represent one species, *A. simus* (Richards *et al.* 1996). What is currently unknown is whether or not the bimodal size distribution in *A. simus* is a result of 2 subspecies or sexual dimorphism.

All extant bears are sexually dimorphic (Stirling 1993a) and this dimorphism increases as species become larger (Stirling & Derocher 1993). For species with a single mate sexual dimorphism is small, whereas in species whose males compete for females, males can be up to 100% heavier (Stirling & Derocher 1993). Kurtén (1967) and others (e.g., Hawksley 1965; Kurtén & Anderson 1980; Cox 1991; Churcher *et al.* 1993; Scott & Cox 1993) have discussed sexual dimorphism in *A. simus*. At Rancho La Brea, contemporaneous large and small forms of this species were recovered, and the largest specimen exceeded the smallest by approximately 25% (Scott & Cox 1993). Though 25% is relatively high, it is still lower than the documented sexual dimorphism in extant *Tremarctos ornatus*, where males are 30-40% larger than females (Saporiti 1949; Stirling 1993a). That sexual

dimorphism alone could account for the size variation in this taxon removes any basis or justification for subspecific distinctions.

The problem with positively distinguishing males from females in the fossil record is that size has been the primary criterion. Though over 100 short-faced bear localities are known, only one site produced a baculum that could belong to a short-faced bear. This was reported from Potter Creek Cave, California, in a compiled list of specimens (Richards *et al.* 1996). The BBC excavation site did not produce a baculum. The lack of recovered *Arctodus* bacula likely reflects both taphonomy and behavior. The majority of skeletal remains representing large individuals are from open sites where only a few elements were recovered (see specimen list in Richards *et al.* 1996). In contrast, horizontal (walk-in) cave passages produced numerous examples of small, yet relatively complete individuals where bacula would likely be found if they had been present. Both the small size of recovered skeletal elements and the lack of bacula from cave deposits suggest that female individuals of *A. simus* were using caves.

The use of caves as dens is relatively common among ursids. In the Americas *Tremarctos ornatus*, *Ursus arctos*, and *U. americanus* use caves for denning when available (Pasitschniak-Arts 1993; Nowak 1999) and polar bears (*Ursus maritimus*) dig their own "caves" in snow (Stirling 1993b). In modern ursids, females spend more time in dens than males. In regions with cold winters, extended periods of denning are an adaptation to seasonal changes in food availability and for birth of tiny cubs incapable of regulating their own body temperature. While denning during the winter months, many ursine species enter a period of dormancy or torpor. All 4 ursid species that live in temperate or Arctic regions enter into a winter sleep (Ramsay 1993). In areas where ursine dormancy occurs, pregnant females enter the dens earlier and leave later. Polar bears are carnivorous and do not undergo winter food shortages like other bears. Because of this, only pregnant females den for extended periods of time (Stirling 1993b). Similarly, in southern populations of *Ursus arctos* and *U. americanus*, males remain active in winter while pregnant females usually den and go into dormancy (Pasitschniak-Arts 1993; Larivière 2001).

In karst regions, fossils of *Arctodus simus* have been recovered almost exclusively from cave sites. In the contiguous United States, 26 of 69 *A. simus* sites (~38%) are in caves (based on data from Richards *et al.* 1996). That greater than one-third of all sites are caves suggests a close association between this species and cave environments. Further, over 70% of the smaller specimens (those assigned as *A. s. simus* by Richards *et al.* 1996) are from cave deposits. Not one of the specimens assigned to the larger morph (*A. s. yukonensis* by Richards *et al.* 1996) is from a cave passage. Taking into account the fact that female ursids are smaller and more prone to den in caves, it seems logical to conclude that the majority of *A. simus* from such deposits were females and may have been denning when they perished.

ACKNOWLEDGMENTS

We would like to thank the landowners, who wish to remain anonymous, for allowing us access to BBC and donating the remains to the Illinois State Museum. This project would not have been possible without the numerous cavers who assisted in the arduous excavations and removal of the remains from the cave, including George Bilbrey, Michael Carter, Amy McCann, Mona Colburn, Jeffrey Crews, Andy Free, Kally Gehly, Matt Goska, Sue Hagan, Dave Matteson, Christy Shannon, Kenny Sherrill, Trevor Stroker, Mick Sutton, Rick Toomey, Ryan Warnol, and David Wronkiewicz. Scott Miller, University of Missouri—Rolla, donated SEM time and instruction. Gary Andrashko, ISM, provided numerous photographs. The CT lab staff at Memorial Medical Center in Springfield IL provided scans and X-rays. Brian Bisbee, ISM, helped with the technical issues associated with the CT scans. Chris Bell and Chris Jass of the University of Texas—Austin, Rufus Churcher - University of Toronto, Greg McDonald - National Park Service, and Ron Richards - Indiana State Museum, provided helpful comments that improved this paper. This project was funded by an Illinois State Museum 1877 Club grant.

REFERENCES

- Christiansen, P., 1999., What size were *Arctodus simus* and *Ursus spelaeus* (Carnivora: Ursidae)? *Annales Zoologici Fennici*, v. 36, p. 93-102
- Churcher, C.S., Morgan, A.V., & Carter, L.D., 1993, *Arctodus simus* from the Alaskan Arctic Slope: *Canadian Journal of Earth Sciences*, v. 30, p. 1007-1013.
- Cox, S.M., 1991, Size range or sexual dimorphism in *Arctodus simus* from Rancho La Brea: Abstract #15, Annual Meeting of the Southern California Academy of Sciences.
- Driesch, A. von den, 1976, A guide to the measurement of animal bones from archaeological sites: Peabody Museum Bulletin 1, Peabody Museum of Archaeology and Ethnology, Harvard University, 137 p.
- Emslie, S.D., 1995, The fossil record of *Arctodus pristinus* (Ursidae: Tremarctinae) in Florida: *Bulletin of the Florida Museum of Natural History*, v. 37, p. 501-514.
- Grayson, D.K., 1989, The chronology of North American late Pleistocene extinctions: *Journal of Archaeological Science*, v. 16, p. 153-165.
- Harrington, C.R., 1991, North American short-faced bears: *Neotoma*, v. 29, p. 1-3.
- Harshyne, W.A., Diefenbach, D.R., Alt, G.L., & Matson, G.M., 1998, Error rates of estimated ages of black bears from tooth cementum annuli: *Journal of Wildlife Management*, v. 62, p. 1281-1291.
- Hawksley, O., 1965, Short-faced bear (*Arctodus*) fossils from Ozark caves: *Bulletin of the National Speleological Society*, v. 27, p. 77-92.
- Hawksley, O., 1986, Remains of Quaternary vertebrates from Ozark caves and other miscellaneous sites: *Missouri Speleology*, v. 26, p. 1-67.
- Hawksley, O., Reynolds, J.F., & Foley, R.L., 1973, Pleistocene vertebrate fauna of Bat Cave, Pulaski County, Missouri: *Bulletin of the National Speleological Society*, v. 35, p. 61-87.
- Hawksley, O., & Weaver, H.D., 1981, Quaternary vertebrates from Carroll Cave, Camden County, Missouri: *Missouri Speleology*, v. 21, p. 199-213.
- Hedges, J., Russell, B., Thrun, B., & White, W.B. 1979, The 1976 NSS standard map symbols: *National Speleological Society Bulletin* v. 41, p. 35-43
- Imes, J.L., Schumacher, J.G., & Kleeschulte, M.J., 1996, Geohydrologic and water-quality assessment of the Fort Leonard Wood Military Reservation, Missouri, 1994-95: U.S. Geological Survey Water-Resources Investigations Report 96-4270.
- Kurtén, B., 1967, Pleistocene bears of North America. 2. Genus *Arctodus*, short-faced bears: *Acta Zoologica Fennica*, v. 117, p. 1-58.
- Kurtén, B., & Anderson, E., 1980, Pleistocene mammals of North America: Columbia University Press, New York, 442 p.
- Lamb, L.M., 1911, On *Arctotherium* from the Pleistocene of Yukon: *Ottawa Naturalist*, v. 25, p. 21-26.
- Larivière, S., 2001, *Ursus americanus*: *Mammalian Species*, v. 647, p. 1-11.
- Marks, S.A., & Erickson, A.W., 1966, Age determination in the black bear: *Journal of Wildlife Management*, v. 30, p. 389-410.
- Merriam, J.C., & Stock, C., 1925, Relationships and structure of the short-faced bear, *Arctotherium*, from the Pleistocene of California: *Carnegie Institution of Washington Publication*, v. 347, p. 1-35.
- Nealson, K.H., Tebo, B.M., & Rosson, R.A., 1992, Occurrence and mechanisms of microbial oxidation of manganese: *Advances in Applied Microbiology*, v. 33, p. 279-318.
- Nealson, K.H., & Stahl, D.A., 1997, Microorganisms and biogeochemical cycles: What can we learn from layered microbial communities?, in Banfield, J.F., & Nealson, K.H., eds., *Geomicrobiology: Interactions between microbes and minerals: Reviews in Mineralogy*, v. 35, p. 5-34.
- Nowak, R.M., 1999, Walker's mammals of the world: Johns Hopkins University Press, Baltimore, 1936 p.
- Pasitschniak-Arts, M., 1993, *Ursus arctos*: *Mammalian Species*, v. 439, p. 1-10.
- Puckette, W., 1976, Notes on the occurrence of the short-faced bear (*Arctodus*) in Oklahoma: *Proceedings of the Oklahoma Academy of Science*, v. 56, p. 67-68.
- Ramsay, M.A., 1993, Winter sleep, in Stirling, I., ed., *Bears: Majestic creatures of the wild*: Rodale Press, Emmaus, p. 68-69.
- Richards, R.L., Churcher, C.S., & Turnbull, W.D., 1996, Distribution and size variation in North American short-faced bears, *Arctodus simus*, in Stewart, K.M., & Seymour, K.L., eds., *Palaeoecology and palaeoenvironments of late Cenozoic mammals: Tributes to the career of C.S. (Rufus) Churcher*: University of Toronto Press, Toronto, p. 191-246.
- Rowe, W.F., 1997, Biodegradation of hairs and fibers, in Haglund, W.D., & Sorg, M.H., eds., *Forensic taphonomy: The postmortem fate of human remains*: CRC Press, New York, p. 337-351.
- Saporiti, E. J., 1949, Contribucion al conocimiento de la biologia del oso de lentos: *Anales de la Sociedad Cientifica Argentina*, v. 147, p. 3-12.
- Schubert, B.W., 2001, Discovery of an ancient giant in an Ozark cave: *The Living Museum*, v. 63, p. 10-13.
- Scott, E., & Cox, S.M., 1993, *Arctodus simus* (Cope, 1879) from Riverside County, California: *PaleoBios*, v. 15, p. 27-36.
- Soibelzon, L., 2002, A general review of the South American Pleistocene short-faced bears (Ursidae: Tremarctinae): Abstract from the 14th International Congress on Bear Research and Management, Steinkjer, Norway.
- Stafford, T.W., Jr., Brendel, K., & Duhamel, R.C., 1987, Study of bone radiocarbon dating accuracy at the University of Arizona NSF Accelerator Radiocarbon Facility for Radioisotope Analysis: *Radiocarbon*, v. 29, p. 24-44.
- Stafford, T.W., Jr., Hare, P.E., Currie, L., Jull, A.J.T., & Donahue, D.J., 1991, Accelerator radiocarbon dating at the molecular level: *Journal of Archaeological Science*, v. 18, p. 35-72.
- Stirling, I., 1993a, The living bears, in Stirling, I., ed., *Bears: Majestic creatures of the wild*: Rodale Press, Emmaus, p. 36-49.
- Stirling, I., 1993b, The polar bear, in Stirling, I., ed., *Bears: Majestic creatures of the wild*. Rodale Press, Emmaus, p. 98-107.
- Stirling, I., & Derocher, A.E., 1993, The behavior of bears, in Stirling, I., ed., *Bears: Majestic creatures of the wild*. Rodale Press, Emmaus, p. 70-83.
- Tebo, B.M., Ghiorse, W.C., van Waasbergen, L.G., Siering, P.L., & Caspi, R., 1997, Bacterially mediated mineral formation: Insights into manganese (II) oxidation from molecular genetic and biochemical studies, in Banfield, J.K., & Nealson, K.H., eds., *Geomicrobiology: Interactions between microbes and minerals: Reviews in Mineralogy*, v. 35., p. 225-266.
- Tedford, R.H., & Martin, J., 2001, Plionarctos, a tremarctine bear (Ursidae: Carnivora) from western North America: *Journal of Vertebrate Paleontology*, v. 21, p. 311-321.
- Voorhies, M.R., & Corner, R.G., 1982, Ice age superpredators: University of Nebraska State Museum, Museum Notes, v. 70, p. 1-4.